Interfacial Electrochemistry of Zn Anodes in Aqueous Electrolytes with Combined Organic Cation and Halide Additives

Sang Hyuk Gong,[ab†] Sunghee Shin,[ac†] Hyo Jin Lim,[ac†] Jin Hwan Kwak,[a] Yiseul Yoo,[ab] In Soo Kim,[d] Puji Lestari Handayani,[e] U Hyeok Choi,[e] Jae Eun Park,[c] Ji Eun Lee,[c] Seuhg-Ho Yu,[c] Kyung Yoon Chung,[af] Sang Kyu Kwak,[*c] Hyung-Seok Kim[*afg]

[a]Energy Storage Research Center, Korea Institute of Science and Technology (KIST), Hwarang-ro 14-gil 5, Seongbuk-gu, Seoul, 02792, Republic of Korea

[b]Department of Materials Science and Engineering, Korea University, 145, Anam-ro, Seongbuk-gu, Seoul, 02841, Republic of Korea

[c]Department of Chemical and Biological Engineering, Korea University, 145, Anam-ro, Seongbuk-gu, Seoul, 02841, Republic of Korea

[d]Nonophotonics Research Center, Korea Institute of Science and Technology (KIST), Hwarang-ro 14-gil 5, Seongbuk-gu, Seoul, 02792, Republic of Korea

[e]Department of Polymer Science and Engineering and Program in Environmental and Polymer Engineering, Inha University, 100 Inharo, Nam-gu, Incheon, 22212, Republic of Korea

[f]Division of Energy & Environment Technology, KIST School, Korea Institute of Science and Technology (KIST), Hwarang-ro 14-gil 5, Seongbuk-gu, Seoul, 02792, Republic of Korea

[g]Yonsei-KIST Convergence Research Institute, Yonsei University, 50 Yonsei-ro, Seodaemun-gu, Seoul, 03722, Republic of Korea

†These authors equally contributed to this work.

*** Corresponding Author**

Correspondence should be addressed to Prof. Sang Kyu Kwak(skkwak@korea.ac.kr) and Dr. Hyung-Seok Kim (hskim0227@kist.re.kr).

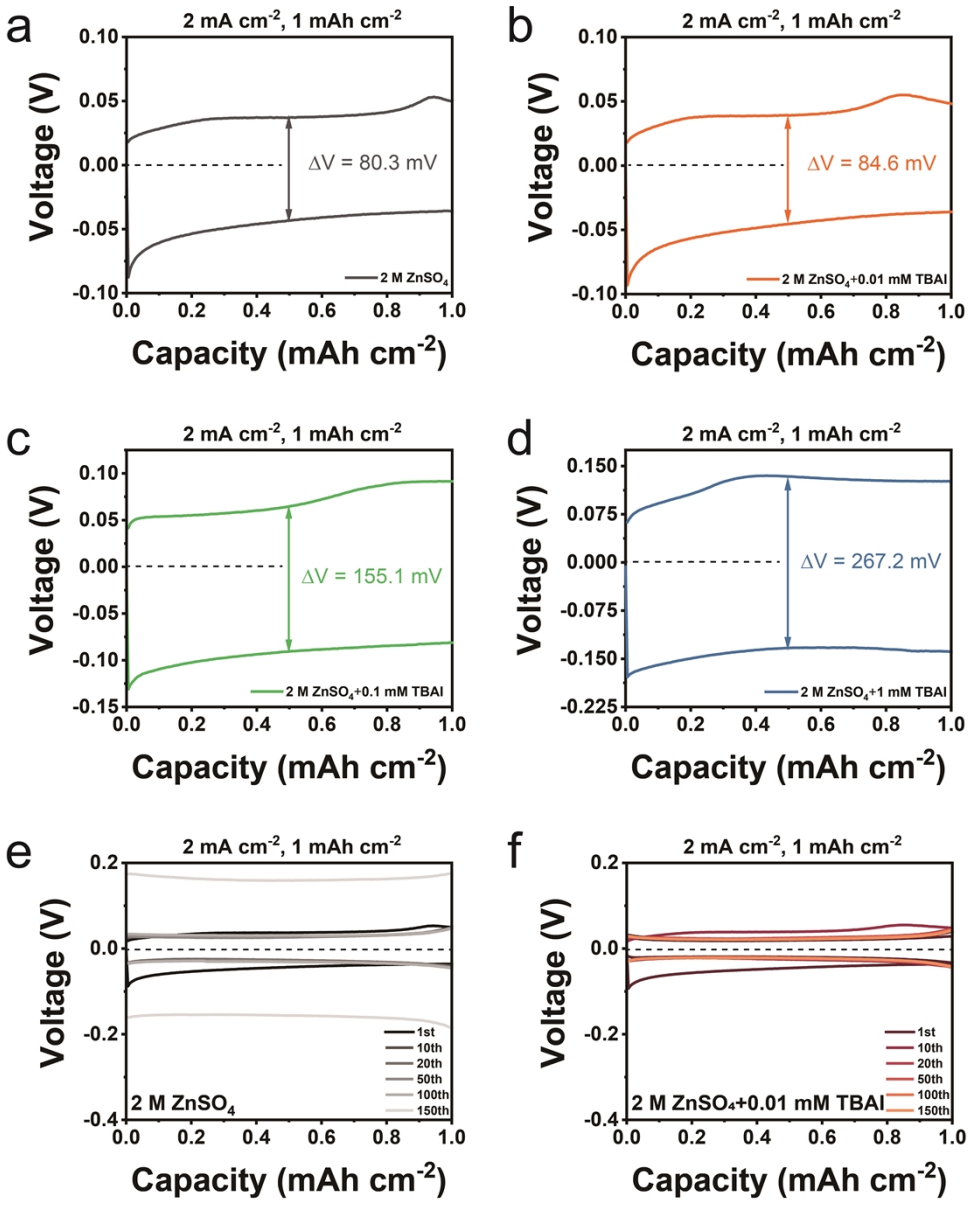

Fig. S1 Voltage profiles of Zn symmetric cells in different electrolytes at a current density of 2 mA cm^{-2} and an areal capacity of 1 mAh cm^{-2}. (a-d) The first cycle plating/stripping overpotential (ΔV) in (a) 2 M $ZnSO_4$, (b) 2 M $ZnSO_4$ + 0.01 mM TBAI, (c) 2 M $ZnSO_4$ + 0.1 mM TBAI, and (d) 2 M $ZnSO_4$ + 1 mM TBAI. (e-f) Long-term plating/stripping voltage profiles at selected cycles (1st, 10th, 20th, 50th, 100th, and 150th) for (e) 2 M $ZnSO_4$ and (f) 2 M $ZnSO_4$ + 0.01 mM TBAI.

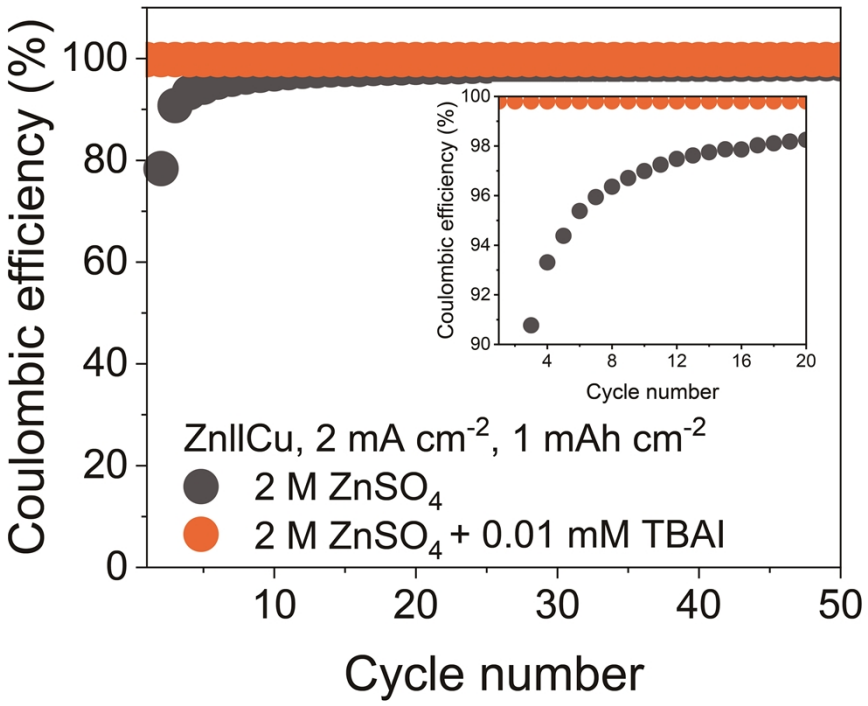

Fig. S2 Coulombic efficiency measurements of Zn||Cu asymmetric cells under different electrolytes (2 M $ZnSO_4$ and 2 M $ZnSO_4$ + 0.01 mM TBAI).

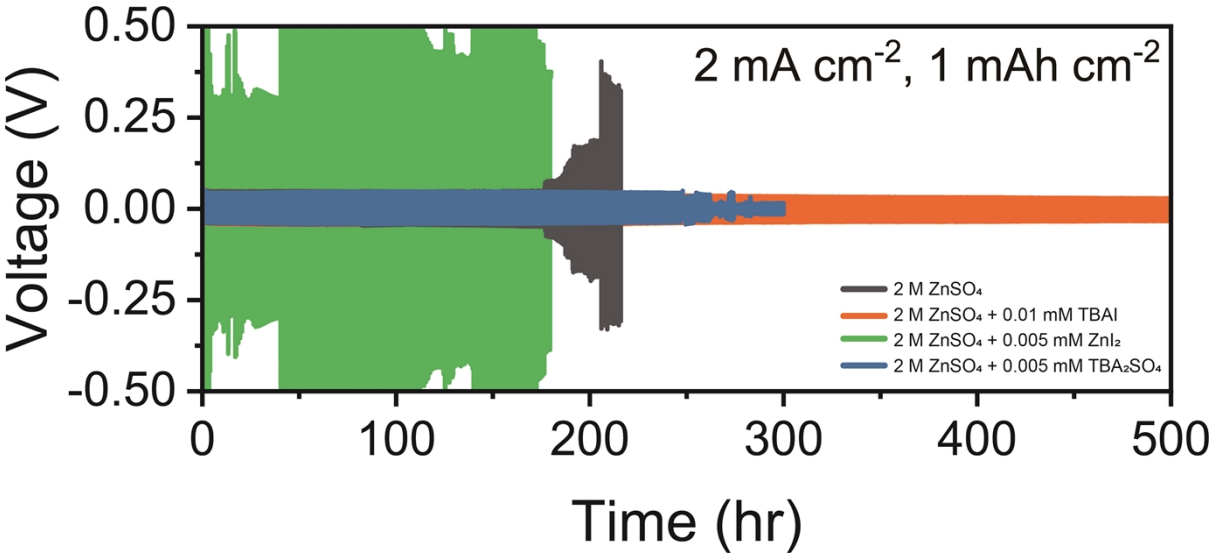

Fig. S3 Long-term cycling performance of Zn symmetric cells at a current density of 2 mA cm^{-2} and an areal capacity of 1 mAh cm^{-2}. The cells were tested in different electrolytes: 2 M $ZnSO_4$ (black), 2 M $ZnSO_4$ + 0.01 mM TBAI (orange), 2 M $ZnSO_4$ + 0.005 mM ZnI_2 (blue), and 2 M $ZnSO_4$ + 0.005 mM TBAI-ZnI_2 (green).

Table S1 Comparison of our work with the amount of additive addition for AZIB in the recent reports.

Additive	Suggested optimal addition amount (g/L)	Ref.
TBAI	0.0037	This work
EDTA	11.7	Ref. 21 in the main text.
Diethyl ether	14.12	Ref 22 in the main text
Polyacrylamide	1	Ref 24 in the main text
Ethylene carbonate	60	Ref 25 in the main text
Mxene	9.48	Ref 16 in the main text
Silk peptide	0.05	Ref 59 in the main text

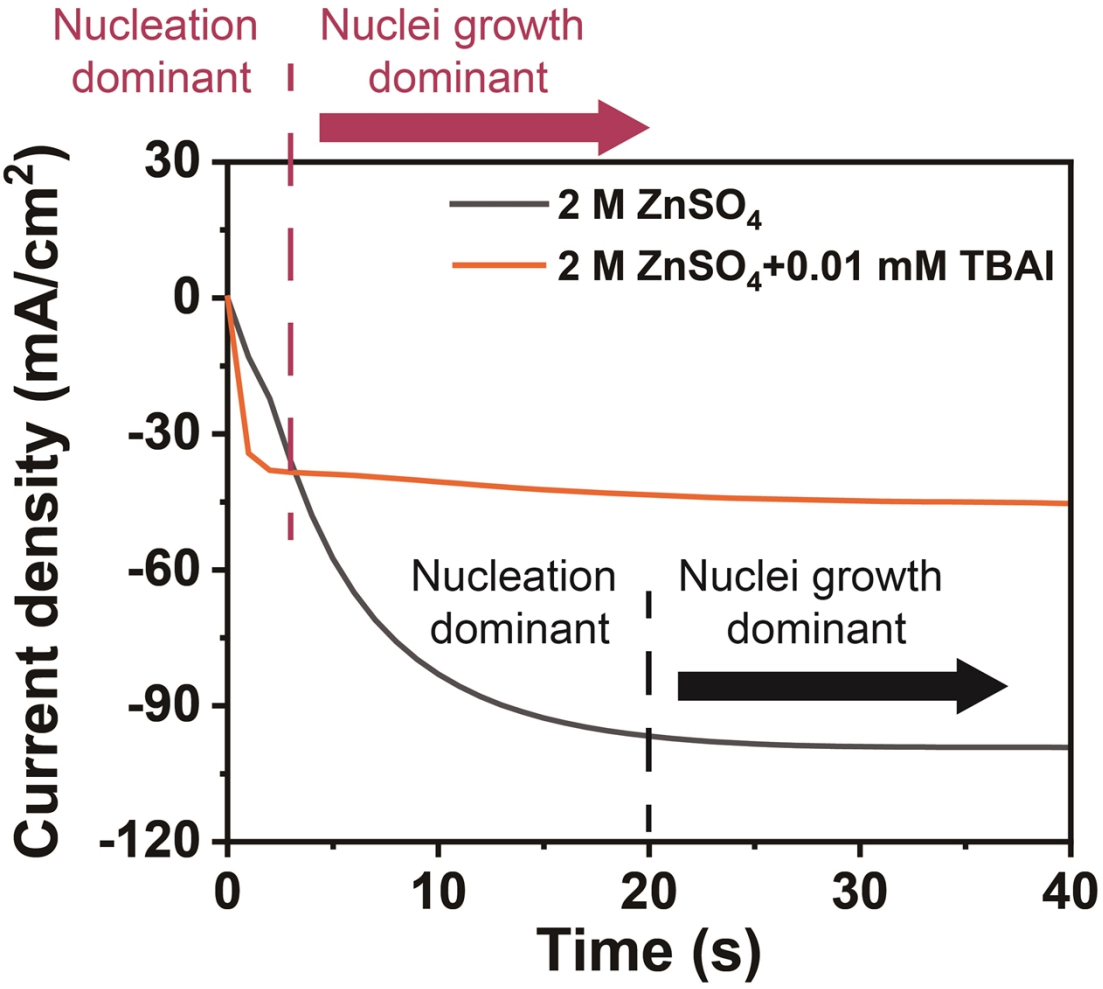

Fig. S4 CA curves of zinc in different electrolytes.

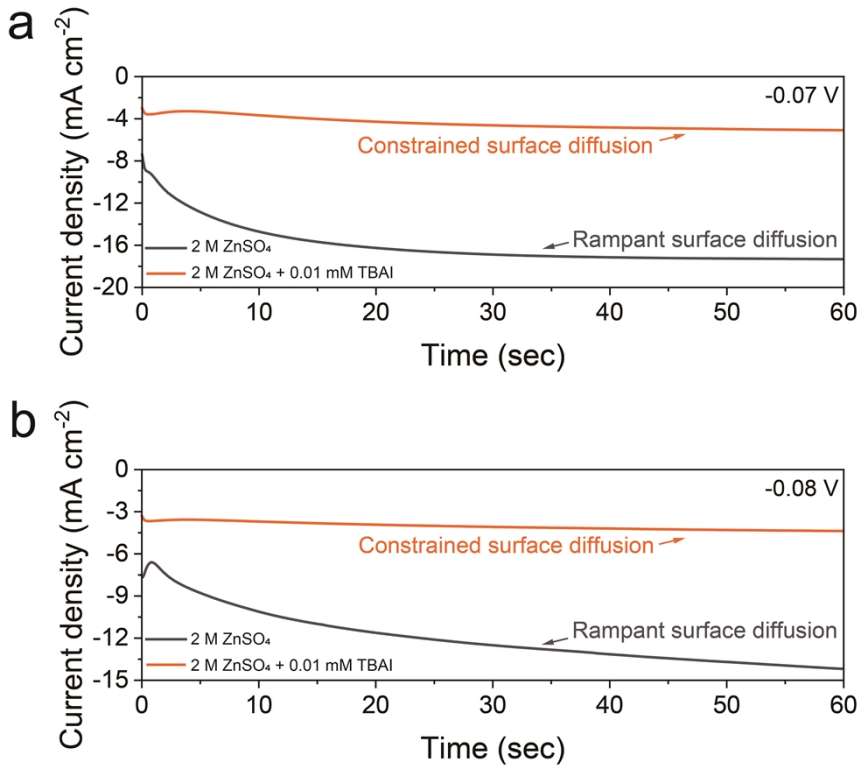

Fig. S5 I-t curves of symmetric cells in the bare electrolyte and 0.01 mM TBAI added electrolyte at (a) -0.07 V and (b) -0.08 V.

$$(\frac{I}{I_m})^2 = \frac{1.9542}{(t/t_m)}\{1 - exp[-1.2564(t/t_m)]\}^2$$ (Instantaneous nucleation) ---------- Equation S1

$$(\frac{I}{I_m})^2 = \frac{1.2254}{(t/t_m)}\{1 - exp[-2.336(t/t_m)^2]\}^2$$ (Progressive nucleation) ---------- Equation S2

I and t are the current density and time, respectively, and I_m and t_m are the maximum values of the current transients.

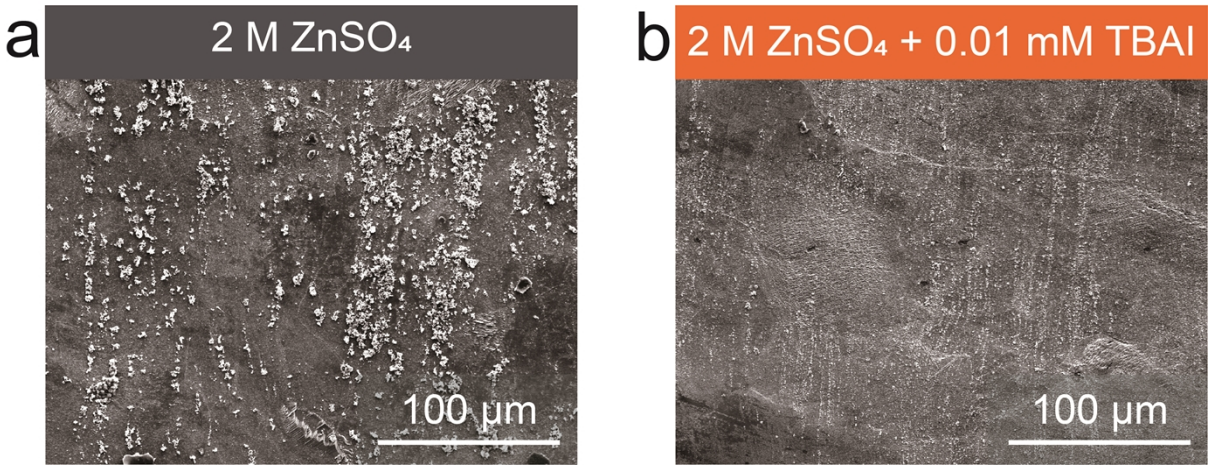

Fig. S6 SEM images of Zn surface after plated at current density of 1 mA cm^{-2} and a specific capacity of 0.1 mAh cm^{-2} in (a) No add and (b) with 0.01 mM TBAI

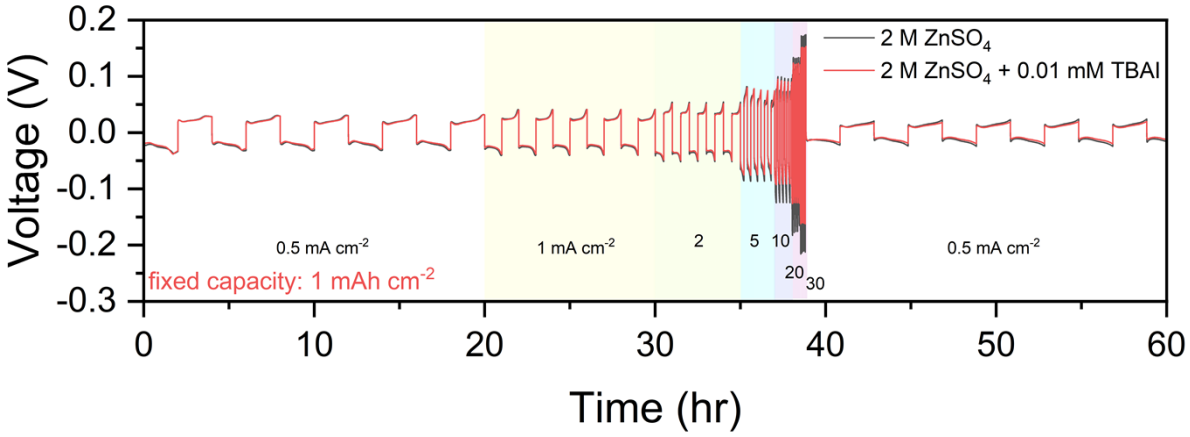

Fig. S7 Rate performance of Zn symmetric cells in 2 M $ZnSO_4$ with and without 0.01 mM TBAI. Cells were cycled at current densities ranging from 0.5 to 30 mA cm^{-2} with a fixed capacity of 1 mAh cm^{-2}. The TBAI-containing electrolyte shows lower polarization and improved stability, especially at high current densities.

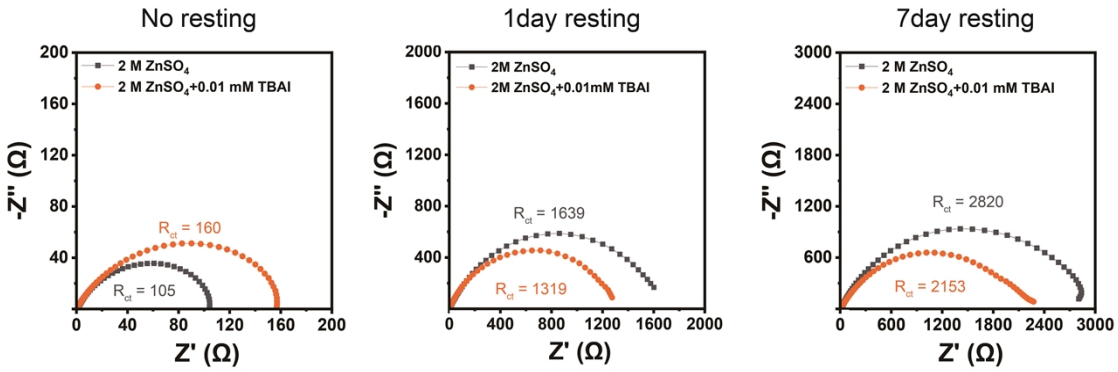

	Before R_{ct} (Ω)	1day resting R_{ct} (Ω)	7days resting R_{ct} (Ω)
2 M $ZnSO_4$	105	1639	2820
2 M $ZnSO_4$ + 0.01 mM TBAI	160	1319	2153

Fig. S8 Nyquist plots of symmetric Zn||Zn cells in 2 M $ZnSO_4$ and 2 M $ZnSO_4$ + 0.01 mM TBAI electrolytes recorded before resting, after 1 day, and after 7 days of resting, together with fitted values of R_{ct}. The control electrolyte exhibited a rapid increase in R_{ct} from 105 Ω to 1639 Ω (1 day) and 2820 Ω (7 days), whereas the TBAI-containing electrolyte remained much more stable (160 Ω initially, 1319 Ω after 1 day, 2153 Ω after 7 days). These results indicate that TBAI addition mitigates interfacial degradation during resting.

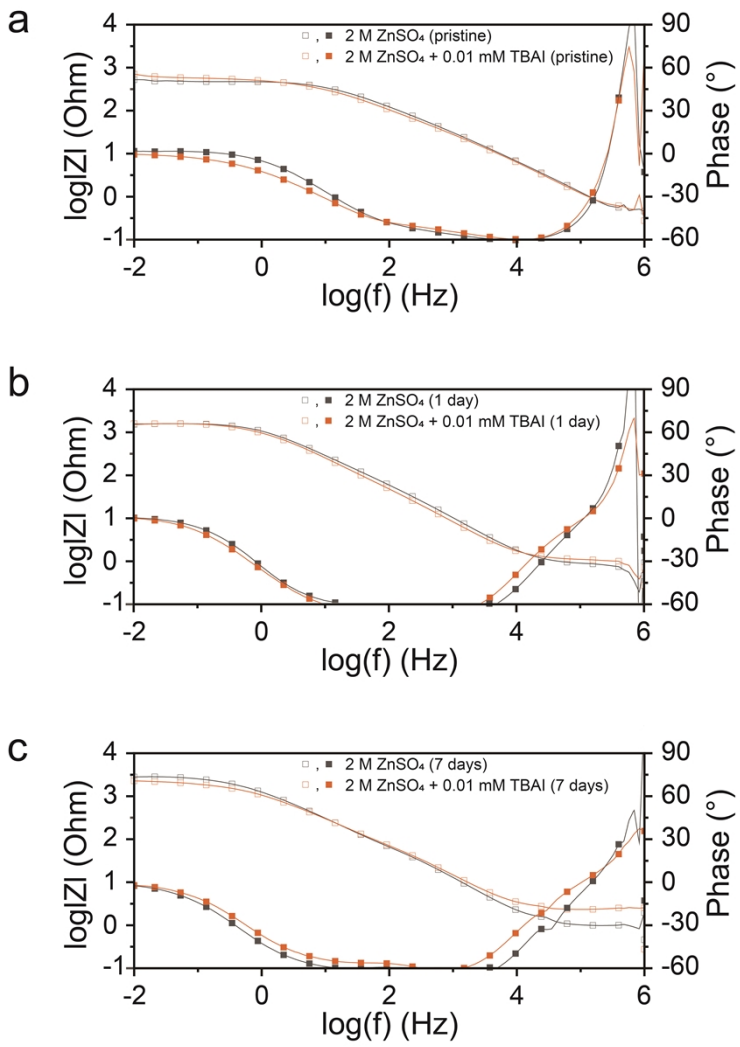

Fig. S9 Bode plots of Zn symmetric cells in 2 M $ZnSO_4$ and 2 M $ZnSO_4$ + 0.01 mM TBAI electrolytes measured after (a) pristine, (b) 1 day, and (c) 7 days of rest. Compared to the bare electrolyte, the TBAI-containing system exhibits consistently lower impedance magnitude and more stable phase angles, even after extended rest. These results confirm that the additive suppresses interfacial degradation by limiting corrosion and by-product accumulation, consistent with the preferential adsorption of TBA^+ on protruding Zn surface sites.

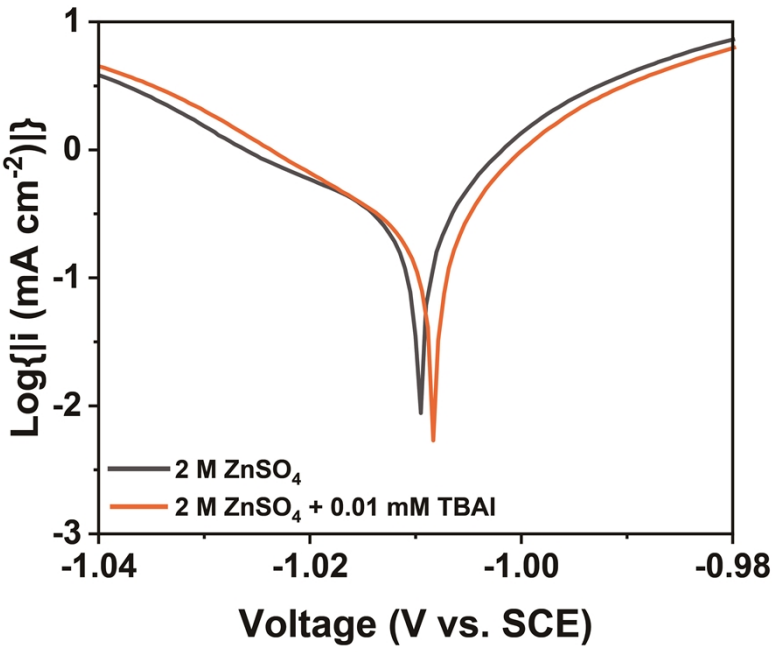

Fig. S10 Tafel polarization curves of 2 M $ZnSO_4$ and 2 M $ZnSO_4$ + 0.01 mM TBAI.

Table S2 Tafel fit corrosion kinetic parameters of Zn symmetric cells without and with 0.01 mM TBAI.

	E_{corr} (mV)	I_{corr} (mA)
2 M $ZnSO_4$	-1.009	2.49
2 M $ZnSO_4$ + 0.01 mM TBAI	-1.008	1.89

E_{corr}: corrosion potential

I_{corr}: corrosion current

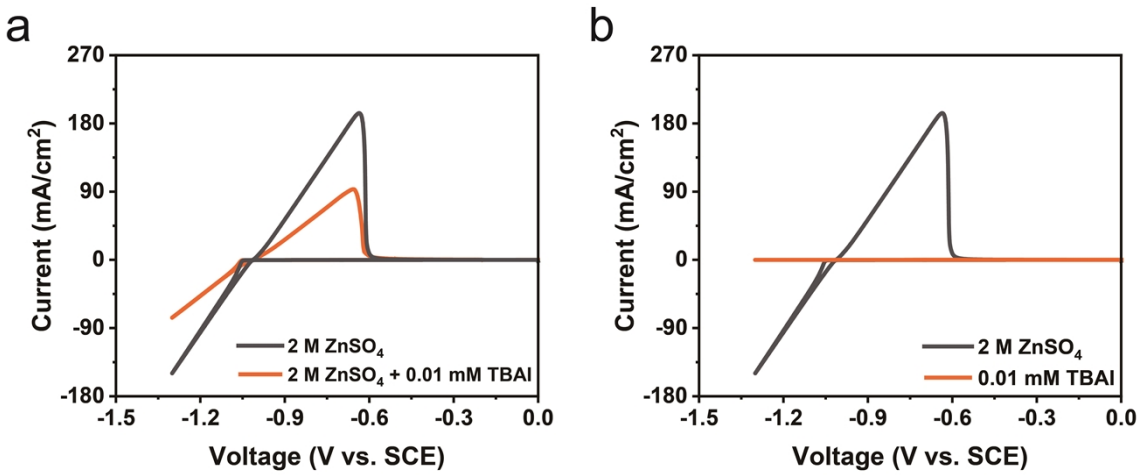

Fig. S11 CV curves for Zn plating/stripping in (a) 2 M $ZnSO_4$ vs. 2 M $ZnSO_4$ + 0.01 mM TBAI and (b) 2 M $ZnSO_4$ vs. 0.01 mM TBAI in water.

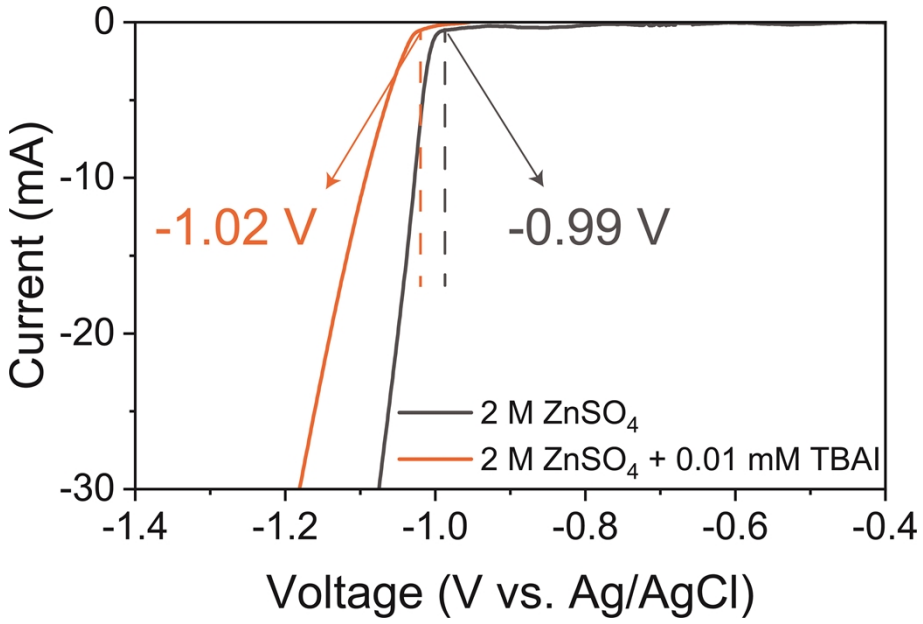

Fig. S12 LSV curves for Zn electrodes in 2 M $ZnSO_4$ (brown) and 2 M $ZnSO_4$ + 0.01 mM TBAI (blue). Measurements were conducted using a three-electrode system with a platinum working electrode (Pt WE), an Ag/AgCl reference electrode (Ag/AgCl RE), and a platinum counter electrode (Pt CE) at a scan rate of 10 mV s^{-1}.

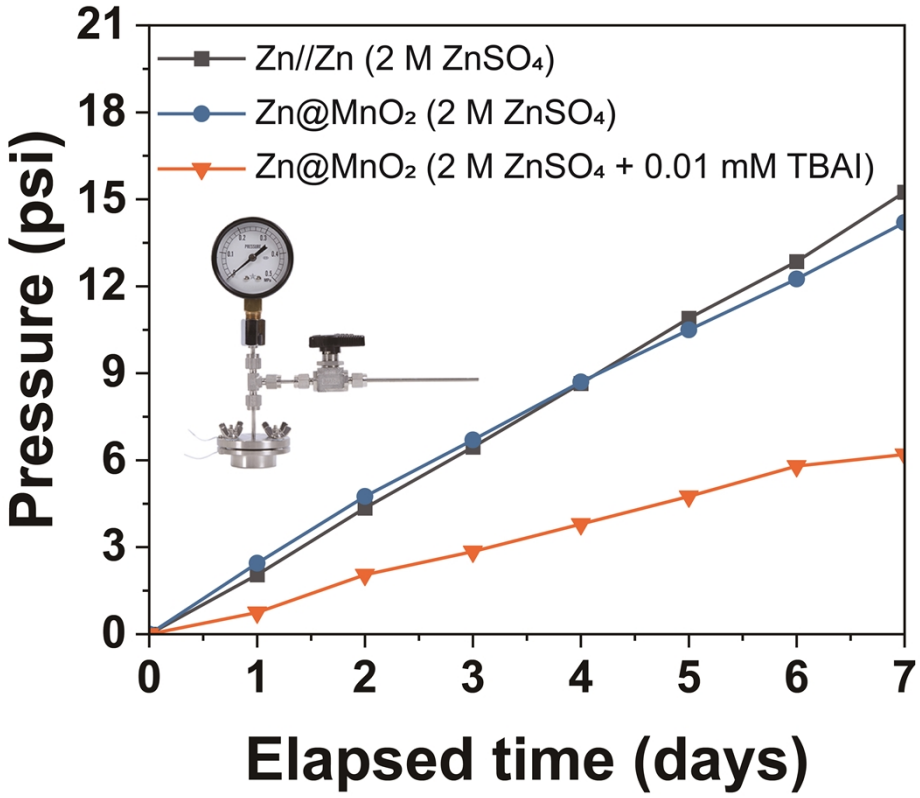

Fig. S13 Change of internal pressure of cells during 7 days after cell fabrication.

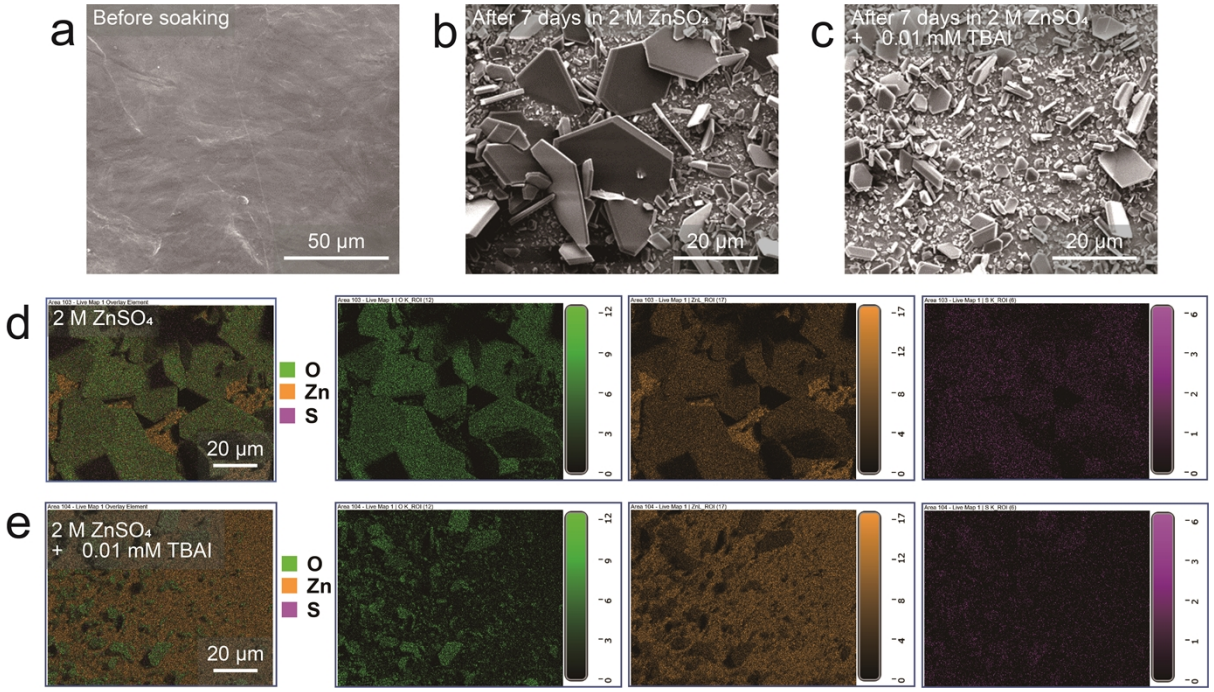

Fig. S14 The SEM images of the Zn surface (a) before soaking, (b) after 7 days in 2 M $ZnSO_4$, and (c) after 7 days in 2 M $ZnSO_4$+0.01 mM TBAI. (d) EDS mapping images of the Zn surface after 7 days soaking in 2 M $ZnSO_4$. (e) EDS mapping images of the Zn surface after 7 days soaking in 2 M $ZnSO_4$+0.01 mM TBAI.

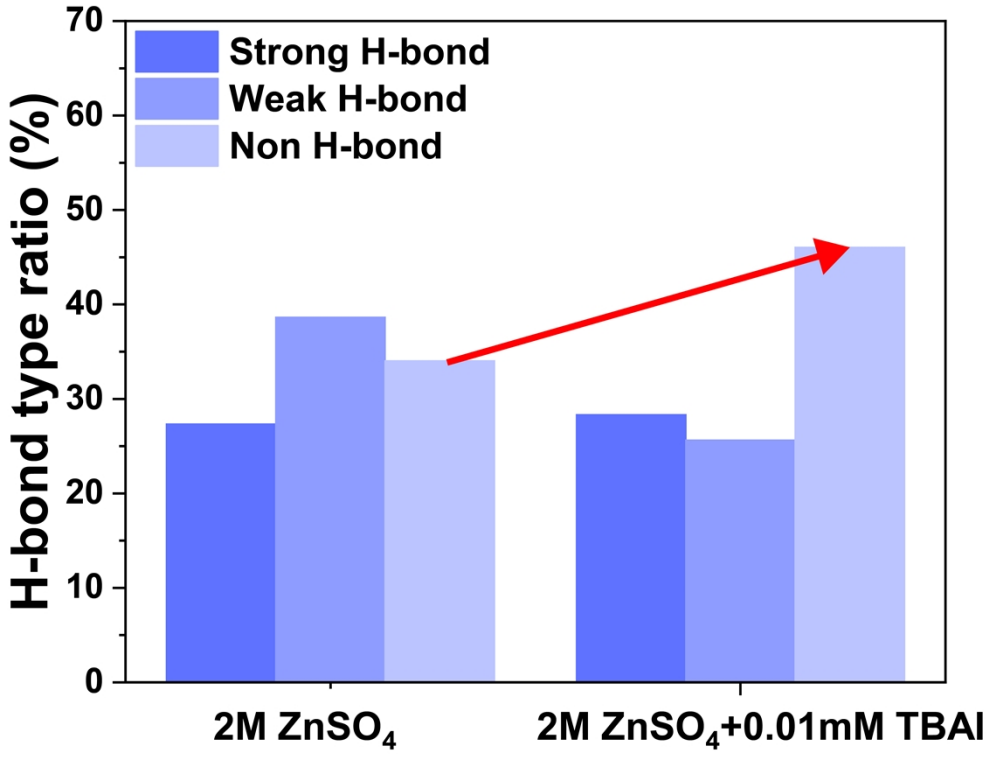

	Strong H-bond area	Weak H-bond area	Non-H bond area
2 M $ZnSO_4$	27.33	38.64	34.03
2 M $ZnSO_4$ + 0.01 mM TBAI	28.32	25.63	46.05

Fig. S15 Water distribution in solution according to the calculated area ratio of Raman spectroscopy.

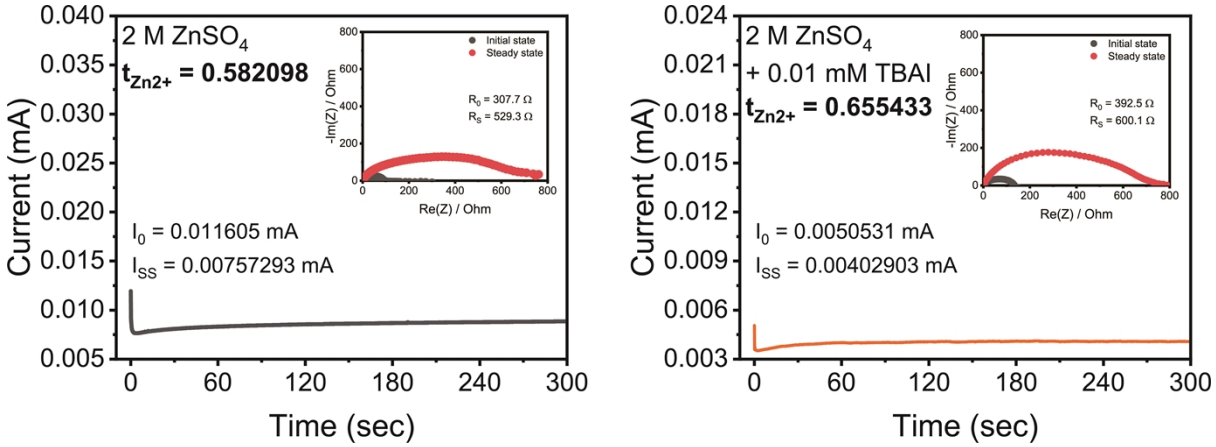

Fig. S16 Chronoamperometric analysis of each electrolyte at an applied voltage of 5 mV (inset: EIS spectra of Zn||Zn symmetric cell with each electrolyte)

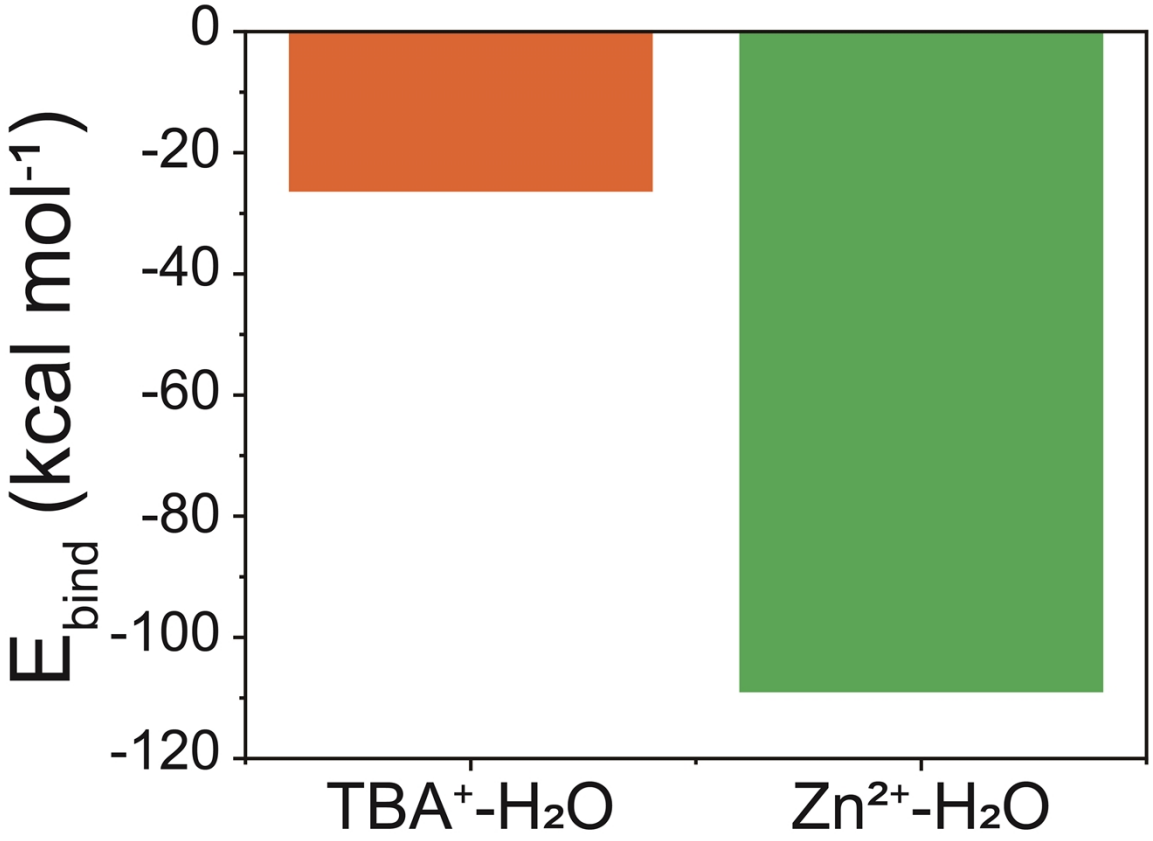

Fig. S17 The calculated binding energy between ions and water.

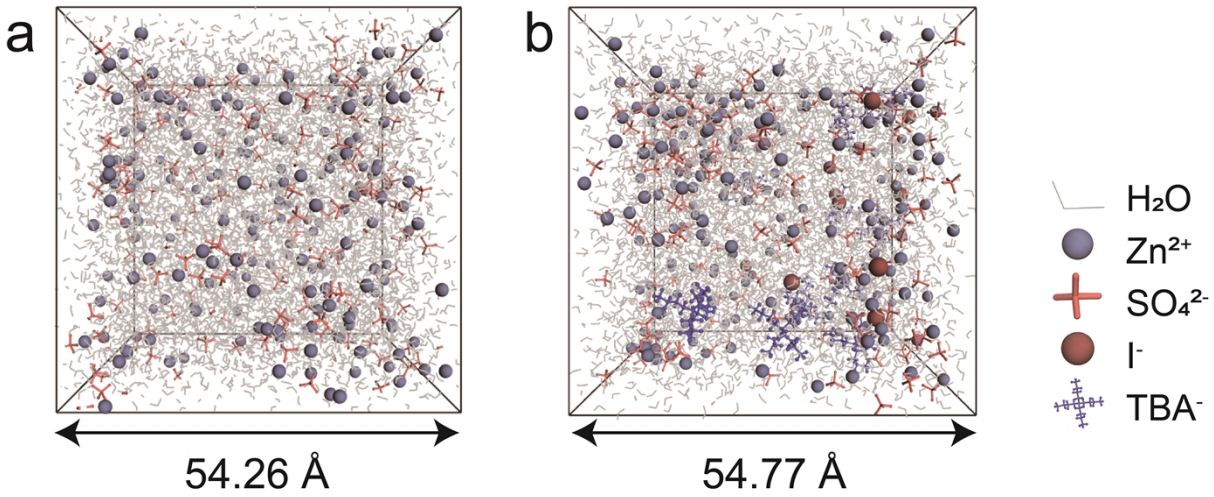

Fig. S18 Snapshots from MD simulations of (a) 2 M $ZnSO_4$ electrolyte and (b) 2 M $ZnSO_4$ with 0.1 M TBAI electrolyte.

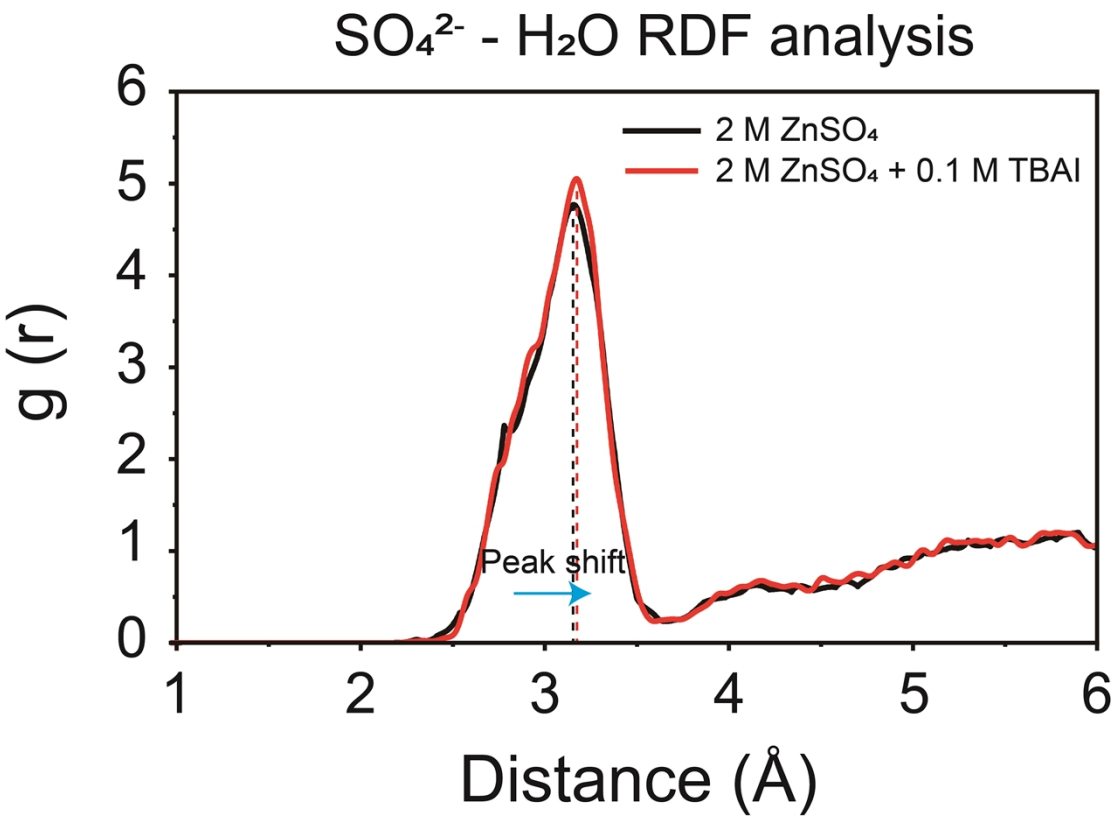

Fig. S19 Radial distribution function (RDF) analysis between SO_4^{2-} and H_2O for 2 M $ZnSO_4$ and 2 M $ZnSO_4$ + 0.1 M TBAI MD simulation system

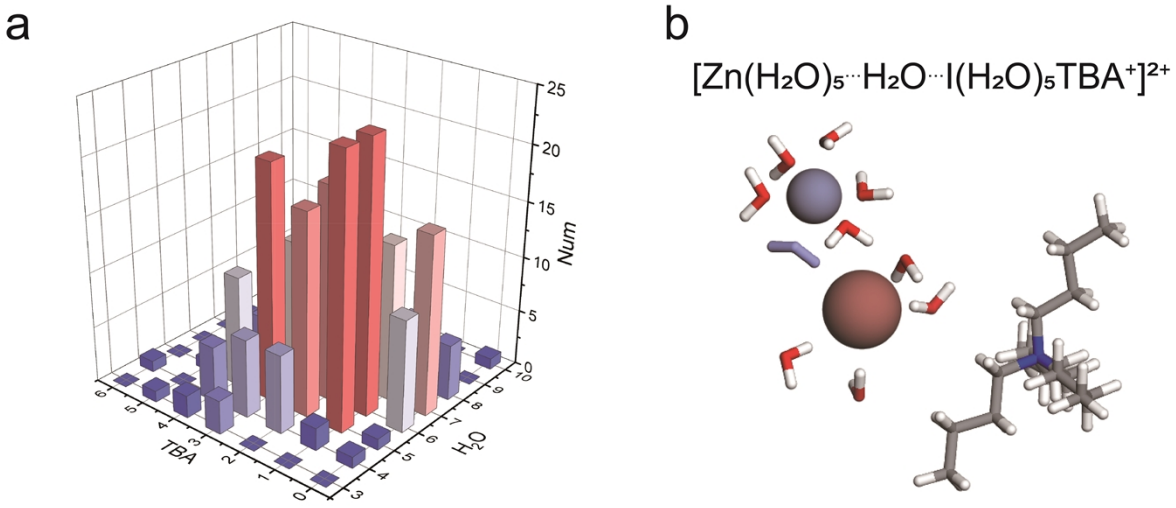

Fig. S20 (a) 3D histogram of the distribution of iodide coordination environment, categorized by the number of coordinating TBA^+ cations and H_2O molecules (b) Representative solvation structure of the predominant iodine coordination state, $[Zn(H_2O)_5\cdots H_2O\cdots I^-(H_2O)_5\cdot TBA^+]^{2+}$. Atoms are colored differently according to the element type: carbon (gray), nitrogen (blue), hydrogen (white), oxygen (red), zinc (navy), and iodine (brown), respectively.

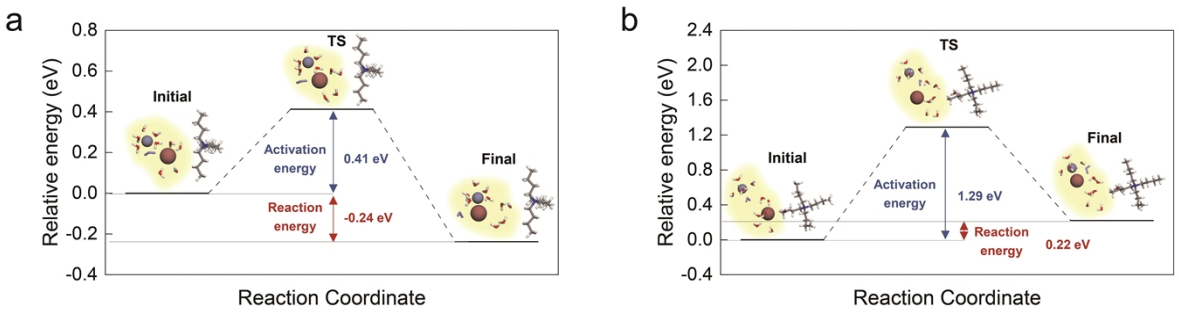

Fig. S21 Energy profile for the structural transition from (a) solvent-shared ion pair (SIP) to contact ion pair (CIP) and (b) solvent-separated ion pair (SSIP) to contact ion pair (CIP). Atoms are colored differently according to the element type: carbon (gray), nitrogen (blue), hydrogen (white), oxygen (red), zinc (navy), and iodine (brown), respectively.

Table S3 Activation and reaction energies for the structural transition from solvent-shared ion pair (SSIP) and solvent-separated ion pair (SIP) to contact ion pair (CIP).

Solvation structure	**SIP to CIP**	**SSIP to CIP**
Activation energy (eV)	0.41	1.29
Reaction energy (eV)	-0.24	0.22

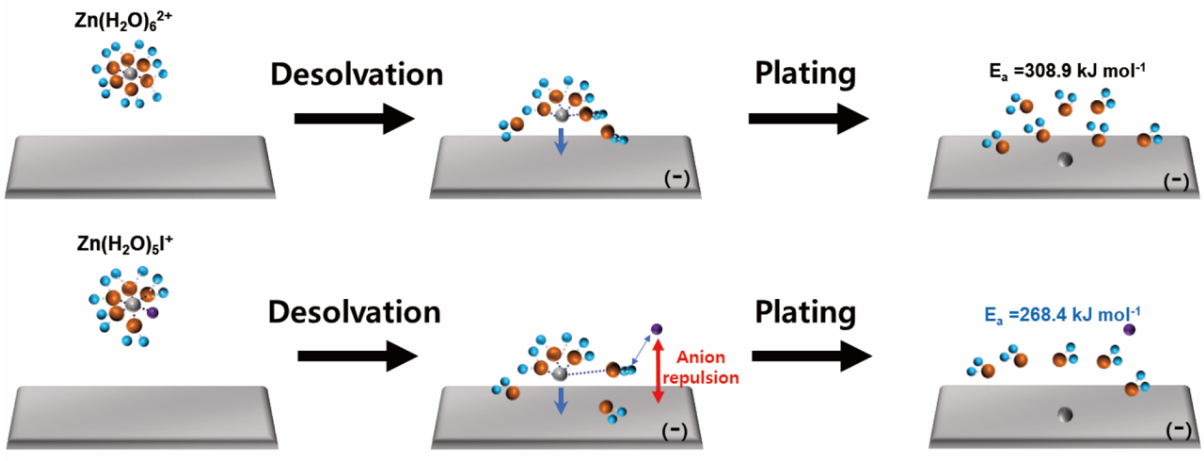

Fig. S22 The desolvation process of the two solvation structures. (a) $Zn(H_2O)_6^{2+}$ in 2 M $ZnSO_4$ electrolyte and (b) $Zn(H_2O)_5I^+$ in 2 M $ZnSO_4$ with TBAI.

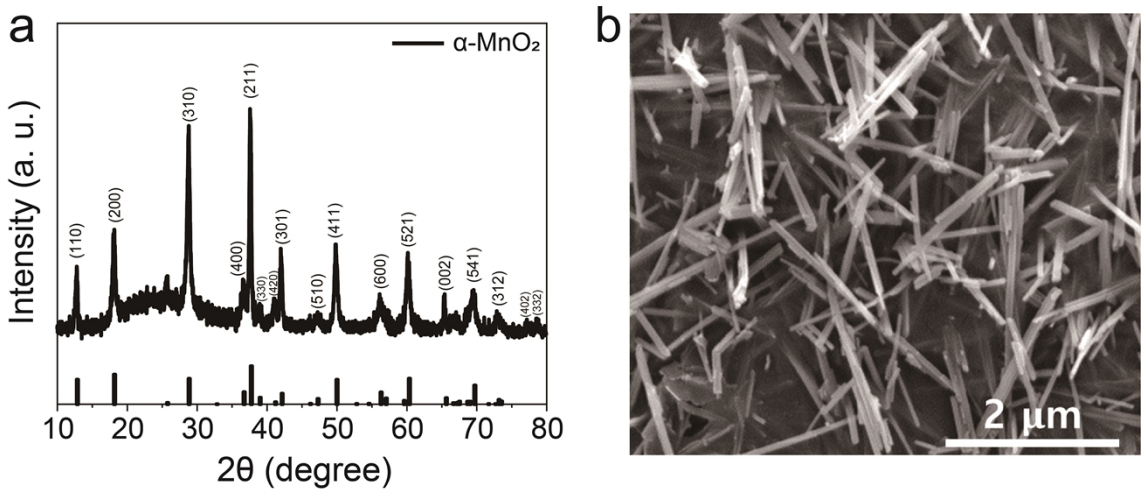

Fig. S23 (a) XRD pattern of synthesized α-MnO_2. (b) SEM image of synthesized α-MnO_2.

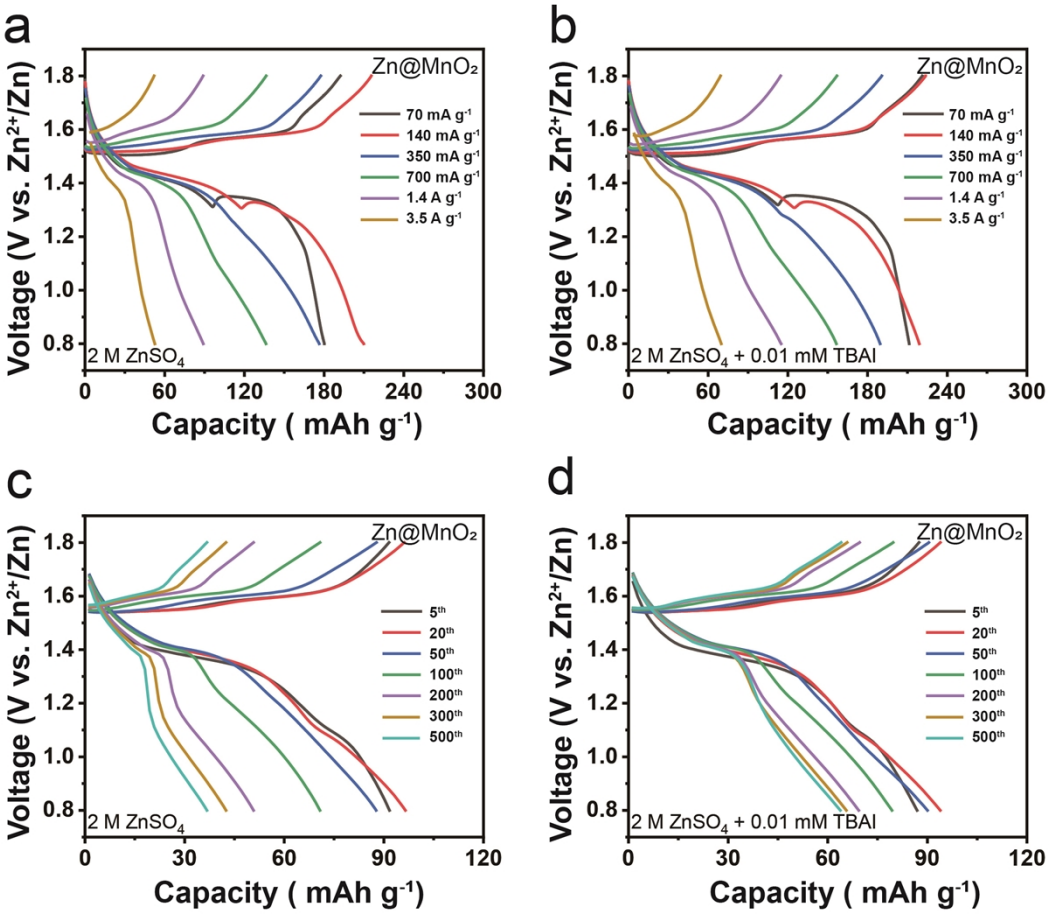

Fig. S24 Voltage profiles of $Zn@MnO_2$ full-cell in (a) 2 M $ZnSO_4$ and (b) 2 M $ZnSO_4$ + 0.01 mM TBAI, at different current densities. Voltage profiles of $Zn@MnO_2$ full-cell in (c) 2 M $ZnSO_4$ (d) 2 M $ZnSO_4$ + 0.01 mM TBAI during cycling.

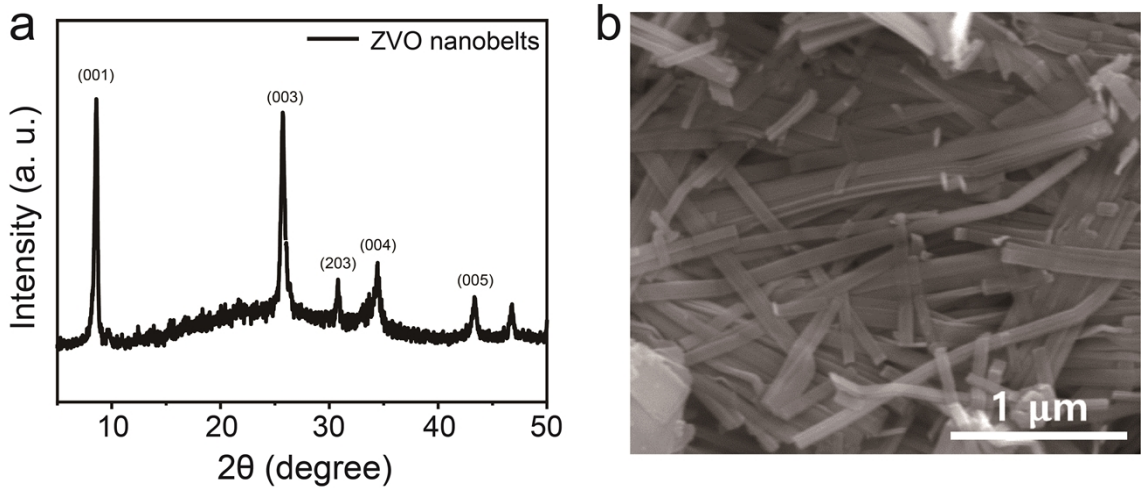

Fig. S25 (a) XRD pattern of synthesized ZVO. (b) SEM image of synthesized ZVO.

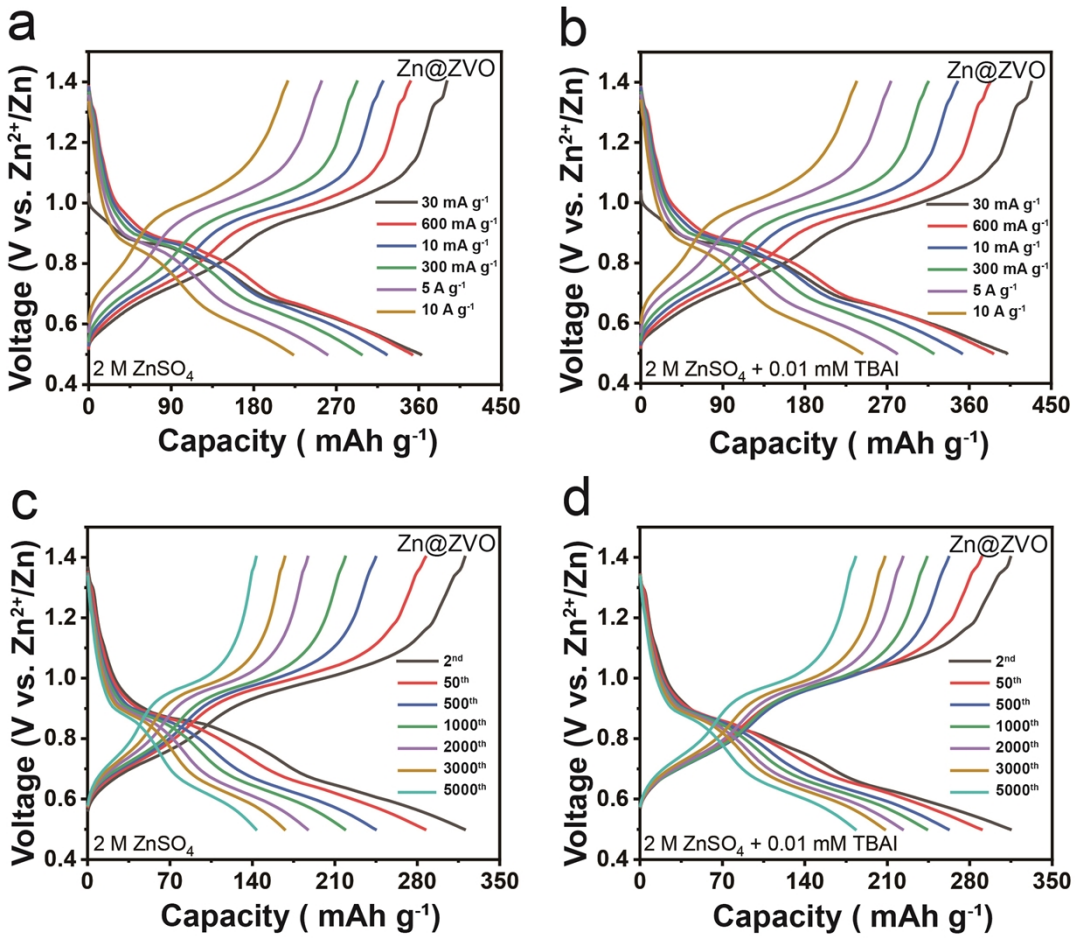

Fig. S26 Voltage profiles of Zn@ZVO full-cell in (a) 2 M $ZnSO_4$ and (b) 2 M $ZnSO_4$ + 0.01 mM TBAI, at different current densities. Voltage profiles of Zn@ZVO full-cell in (c) 2 M $ZnSO_4$ (d) 2 M $ZnSO_4$ + 0.01 mM TBAI during cycling.

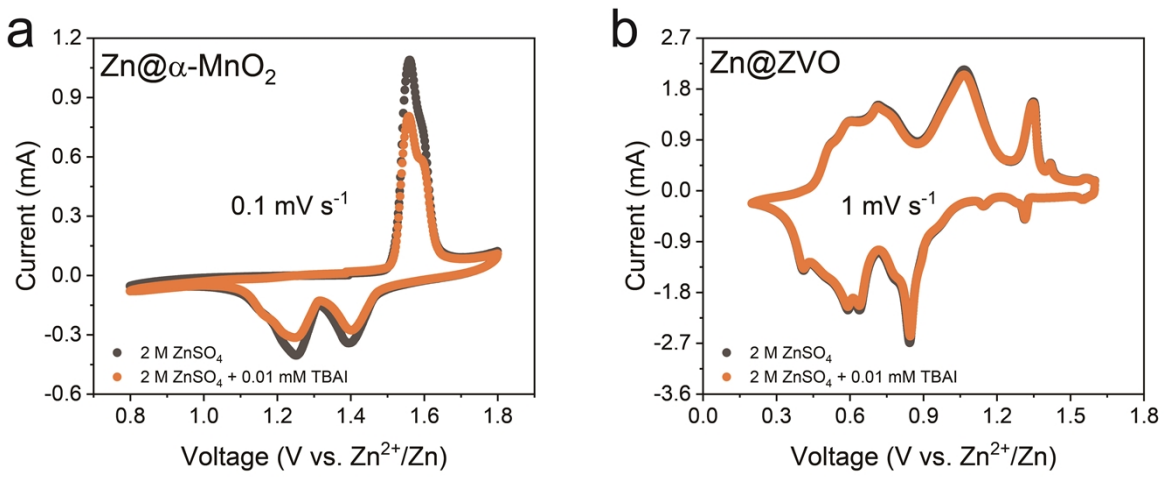

Fig. S27 Cyclic voltammetry (CV) curves of Zn@α-MnO_2 (a) and Zn@ZVO (b) full cells in 2 M $ZnSO_4$ with and without 0.01 mM TBAI.

The addition of TBAI leads to reduced peak polarization and enhanced current response in both systems, suggesting improved redox kinetics and electrochemical reversibility. The consistent trend across different cathode materials indicates that the performance enhancement originates from the stabilized Zn anode interface rather than cathode-specific effects.